Journal Homepage: - www.journalijar.com
INTERNATIONAL JOURNAL OF ADVANCED RESEARCH (IJAR)
Article DOI: 10.21474/IJAR01/2357
DOI URL: http://dx.doi.org/10.21474/IJAR01/2357
ISSN NO. 2320-5407

RESEARCH ARTICLE

VOLUME-BASED SPECTRUM SENSING FOR COGNITIVE RADIO USING MULTIPLE ANTENNAS.

B.Swarna Kumar[1] and C. Subhas[2].
1. M. Tech (DECS), Sree Vidyanikethan Engineering College.
2. Professor in ECE & Dean (Academics), Sree Vidyanikethan Engineering College.

Manuscript Info

Manuscript History

Received: 18 October 2016
Final Accepted: 20 November 2016
Published: December 2016

Key words:-
Cognitive Radio, Spectrum Sensing, Volume-based method, Gamma distribution.

Abstract

In this paper, we consider the use of Spectrum Sensing. The noise and primary user signal assumed as independent complex zero-mean, Gaussian random variables. The volume-based method for Spectrum sensing is analyzed, it can provide the properties of constant false alarm rate, and free of noise uncertainty.
By comparing first and second moments for signals active and signals-deactivate hypothesis together with using Gamma distribution approximation and derive false alarm and detection probabilities.
In the sense of detection performance, we compare Proposed method, Hadamard ratio test, AGM, John's method and ED.

Introduction:-

Cognitive radio(CR) defined as an intelligent wireless communication system, it provides more proficient transmission by allowing Secondary Users(SUs) to utilize the unused spectrum segments. The spectrum management is composed of four major steps as defined in [1]: sensing, decision making, sharing, and mobility. Among these, the SS and decision making are the most important constituents for the establishment of CR networks. CR users should detect the Primary user (PU) systems to find the spectrum holes or unused spectrum to utilize them effectively cognitive access. At the same time, they should prevent interference to the PUs due to their cognitive access of the channels [2].

It has unburdened in [3] that the current policies of fixed spectrum allocation do not fully utilize the available spectrum.

CR, whose main idea is to sense the spectrum over a wide range of frequency bands and use the temporally unengaged groups for capable wireless transmission. It is a promising epitome to increase the spectrum manipulation efficiency. In a CR network, when the vast cycle resources of a PU not occupied, an SU is legitimate to use them. That is to say, and the SU desires to perceive the occurrence of the PU scrupulously. The Generating as a binary hypothesis testing problem and is particularly challenging for small sample size and low signal-to-noise ratio (SNR) circumstances.

For the situation of signal absence, the noticed data only consist of noise and are usually given to be, Independent and identically distributed (IID). It is perceptible that the energy and correlation structure of the observations differ when the PU signal is present [4]. As a result, spectrum sensing can be concluded by making use of these dissimilarities. When the noise power is known, the energy detector(ED) [6,] has been shown to be optimal for the IID PU signals. The eigenvalues of the obtained signal sample covariance matrix (SCM) in the signal occurrence

Corresponding Author:- B. Swarna Kumar.
Address:- M. Tech (DECS), Sree Vidyanikethan Engineering College.

situation are more spread out than those in the noise only case, which corresponds to a scaled identity matrix in the asymptotic sense. The spread-out Eigen-spectrum results from the connection contraction characteristic in the covariance matrix. As a consequence of many eigenvalues-based detectors which exploit the correlation for spectrum, sensing has been proposed in the literature [13]. Derived the framework of generalized likelihood ratio test (GLRT) [16], the arithmetic-to-geometric mean (AGM) method [17] can identify reliably the correlated signals embedded in IID noise. AGM algorithm has its root in the maximum likelihood (ML) theory which turns out to be inefficient when the temporal and spectacular amplitude are tiny, that is, the hypothetical verdict threshold cannot be precisely indomitable. On the other hand, the maximum-to-minimum eigenvalues (MME) approach is heuristically developed to test if the SCM corresponds to a particularity conditions or its applicator alternative with the use of its greatest extent and smallest amount eigenvalues. Since not all Eigen- values are occupied, its exposure enactment is incredibly perceptive to weak applicatory signals and tiny samples scales. Moreover, the reckoning of the hypothetical threshold for the MME algorithm relies on the dispersion of the limit and smallest eigenvalues in the structure of random matrix theory (RMT) [18]. In practice, the SU receivers are usually uncelebrated, making the noises at different antennas to be non- uniform.

Some approaches have suggested for robust SS in the literature, such as the GLRT test [18], independence test [17], Hadamard ratio test, locally most important invariant test(LMPIT)[17] and volume-based approaches [19]. The underlying idea is that the determinant of SCM or volume differs dramatically between the signal absence and signal-presence situations It is worth pointing that the volume-based detector developed [18] for real-valued observation, and its detection enactment has not yet been critiqued, which is the officer involvement of these work. By comparing first and second consequences of signal absence and signal-presence hypothesis simultaneously with using the Gamma distribution approximation, we originate accurate analytic formulae for the false alarm and detection probabilities for the situation of IID noise. It enables us to develop the theoretical decision threshold for possible primary signal detection as well as receiver operating characteristic (ROC) for performance evaluation.

The rest of the paper organized as follows. The problem formulation of spectrum sensing conferred in section II. Volume-based determined in section III. Simulation results presented in section IV. Conclusions presented in section V.

Problem Formulation:-

Signal model:-

Consider a multipath fading channel model and assume there 1 PU and (d-1) interference users with d >=1, and each of them equipped along with a single antenna in a CR network. The intervention users are now counted as PUs because they cover the same channel, that is, there are *d* PUs. To find the temporally unoccupied channel, an SU receiver with *M* antennas desires to scrutinize this channel. Denote the signal absence and signal-presence hypothesis by H_0 and H_1, respectively.

SU with *M* antennas tries to detect the signals emitted by *d* PUs with the single antenna.

$$X_t=H\,S_t + n_t \qquad (1)$$

Here $H \in C^{M\,X\,d}$ denotes the channel matrix between the PUs and SU, which is stranger deterministic throughout the wise period, and the

$$X_t =[x_1(t) ,\ldots\ldots x_M(t)]^T \qquad (2)$$

$$S_t =[S_1(t),\ldots\ldots..S_d(t)]^T \qquad (3)$$

$$n_t =[n_1(t) \ldots\ldots.,n_M(t)]^T \qquad (4)$$

and the consideration, signal, and noise vectors, correspondingly, with $(.)^T$ being transposed operator. We assume that sounds are statically independent and satisfy $_{Si}(t) \sim N(0,\sigma^2_{Si})(i=1,\ldots.,d)$ with σ^2_{Si} being the *i*th unknown signal variance, and that $_{Ni}(t) \sim N(0, T_i)$ $(i=1\ldots.M)$ with T_i being the unknown noise variance. In signal –absence hypothesis H_0, the population covariance matrix of the observation x_t is $\Sigma=E[x_t\, x_t^H]=\text{diag}\,(T_1\ldots.T_M)$.

However, presence of primary signals destroys this diagonal structure, leading to

$$\Sigma= H\,\Sigma_s H^H +\text{diag}(T_{1\ldots.}T_M) \qquad (5)$$

Here $\Sigma_s=E[S_t S_t]$.

When signal absence and signal presence SS issues cast as the binary hypothesis test, there four it can be written as

$$H_0=\Sigma = \text{diag}(T_{1,\ldots.}T_M) \quad (6)$$

$$H_1=\Sigma > \text{diag}(T_{1,\ldots.}T_M) \quad (7)$$

Here H_0 is denoted as signal absence and H_1 is denoted as signal presence.

Sensing solution:-

Σ is the hyper volume of the geometry determined by the row vectors of Σ. For example, let us consider the scenario of three receiving antennas where the observed data with zero mean and unity variance may be independent, correlated or coherent.

Here corresponding covariance matrices are the 3x3 identity matrix, full rank matrix, and list one arbitrary pattern. For namesake, it can be called as the cube, parallelepiped, and line. It formed by the row vectors of the matrices is drawn in Fig.1.

Here, the volume of the cube, parallelepiped, and line, are denoted by v_1, v_2, and v_3, in the sense of cube represented as absence signal situation, whereas parallelepiped and line can represent a signal present case. For signal-absence situation, the covariance matrix is a 3x3 identity matrix, that is $v_1=1$, and signal presence situation $v_2 < v_1$, $v_1 =0$.

Here to utilize the correlation structure for practical spectrum sensing, we need to calculate the sample covariance matrix(SCM) rather than the population covariance matrix Σ; it represented as

$$S = \frac{1}{N}\sum_{t=1}^{N} x_t\, x_t T \quad (8)$$

And the volume of geometry with unity edge is $|D^{-(1/2)}S\, D^{-(1/2)}|$, consequently we have

$$\xi_{VOL} \triangleq \frac{|S|}{|D|} \quad (9)$$

For the situation of signal absence, $|D^{-(1/2)}S\, D^{-(1/2)}|$ asymptotically get the identity matrix as the number samples tend to infinity, leading the volume of one. For the situation of signal presence, the correlation structure gets leads to the notable reduction of the total amount. So we compare the predetermined threshold and volume of the geometry,

$$\xi vol \underset{H_1}{\overset{H_0}{\gtrless}} \Upsilon vol \quad (10)$$

Here volume-based detector offers the same expression as the Hadamard ratio test but with a different diagonal matrix in the denominator. The Hadamard ratio rules given below

$$\varepsilon_{\circ} HDM \triangleq \frac{|S|}{|G|} \underset{H_1}{\overset{H_0}{\gtrless}} \Upsilon HDM \quad (11)$$

In this configuration, Υvol is approximately equal to the $\varepsilon_{\circ} hmd$.

On another hand, ${}_{i}PI$ is much larger than the ${}_{iiRII}$ due to the correlation, making ξvol much smaller than $\varepsilon_{\circ} hmd$ under H_1.

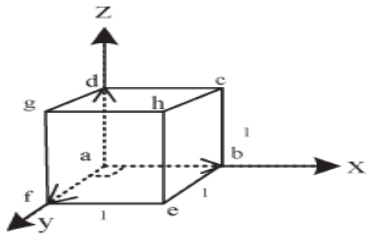

(a)

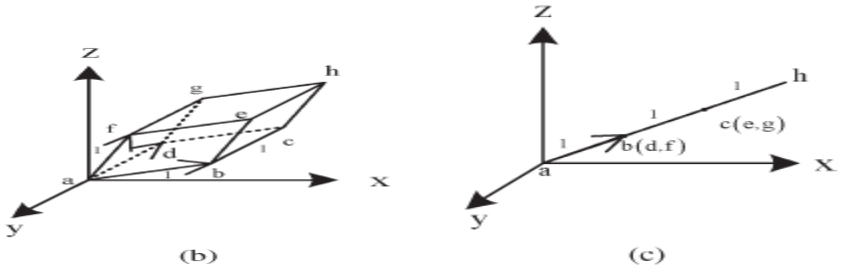

Fig 1:- Volume comparison for uncorrelated, correlated, coherent (a) v_1=1; (b) $v_2 < v_1$ (c) v_1=0.

To consider the different behaviors of the volume-based and Hadamard ratio approaches, the empirical probability density functions (PDFs) of the test statistics for these two methods plotted in fig.2. In this configuration we are taking four antennas, three primary signals with powers [-2,-3, -4] Db are assumed to exist in the sensed channel, and the noise is IID with unity power. In fig.2(a), the number samples sufficiently large. Here N=5000, so that the SCM is the very accurate estimate of the population covariance matrix, and for absent signal situation, the covariance matrix is an identity matrix, it means that volume-based method is approximately equal to the Hadamard ratio, as drawn in fig. 2 (a). It seemed that the PDF under H_1, denoted as p_1, is much further away from the PDF under H_0, denoted as p_0, volume based detector than that of the Hadamard ratio rule. When the number samples become small, like *N=50,* the SCM is the inaccurate estimate of the population one. These numerical results represented in fig.2(b).The thereby implies that the volume-based algorithm can detect the PUs correctly with higher probability than the Hadamard ratio approach especially in the small sample and low signal to noises ratio situations.

In theoretical analysis, the volume-based test statics is modified as

$$\varepsilon_{\zeta} \triangleq -log\frac{|S|}{|D|} \underset{H_1}{\overset{H_0}{\gtrless}} \Upsilon \qquad (12)$$

Here Υ is the decision threshold of the volume-based detector, the next section, derived the Gamma distribution approximation, accurate analytic formulae derived for false alarm probability, detection probability, the theoretical decision threshold as well as ROC. It enables us accurately to determine the theoretical decision threshold for the practical SS.

Performance analysis;-

In this one, the analytic formula for the false-alarm probability, detection probability, decision threshold as well as ROC is derived by assuming the additive noise is IID.

Here we are trying to first and second moments under the signal activation hypothesis and signal deactivation theory, and first, we derived the Detection probability of the volume-based method.

Detection Probability:-

Let us considered the $p_1(y)$ be the PDF of the statistic variable ξ under presence signal hypothesis (H_1), which is determined the following proposition.

Preposition 1:-

For number of antennas *M* and sample numbers *N* with *N≥M,* the first moment Gamma approximation to the PDF of ξ under signal presence hypothesis(H_1) is

$$P_1(y) \cong \frac{y\alpha 1-1\beta 1-\alpha 1e-y/\beta 1}{\Gamma(\alpha 1)}\ , \ y\varepsilon[0,00] \qquad (13)$$

Here $\Gamma(.)$ is a complete function.

$$\alpha 1 = \frac{\mu_1^2}{v_1^2} \qquad (14a)$$

$$\beta_1 = \frac{v_1^2}{\mu_1} \qquad (14b)$$

μ_1 and ν_1 being the second order approximation to the mean of ξ and the first-order approximations to the variance of ξ. Detection probability is computed as

$$P_d(\Upsilon) \triangleq Prob(\xi<\Upsilon | H_1) = F(\Upsilon;\alpha_1,\beta_1) \quad (15)$$

Provide that the population covariance matrix Σ gave, and
$F(\Upsilon;\alpha_1,\beta_1)$ is the cumulative distribution function (CDF) of Gamma distribution. From the constant false-alarm rate(CFAR) perspective, the decision threshold Υ usually is determined under the absence signal hypothesis, it must be resolute and independent of the noise variance.

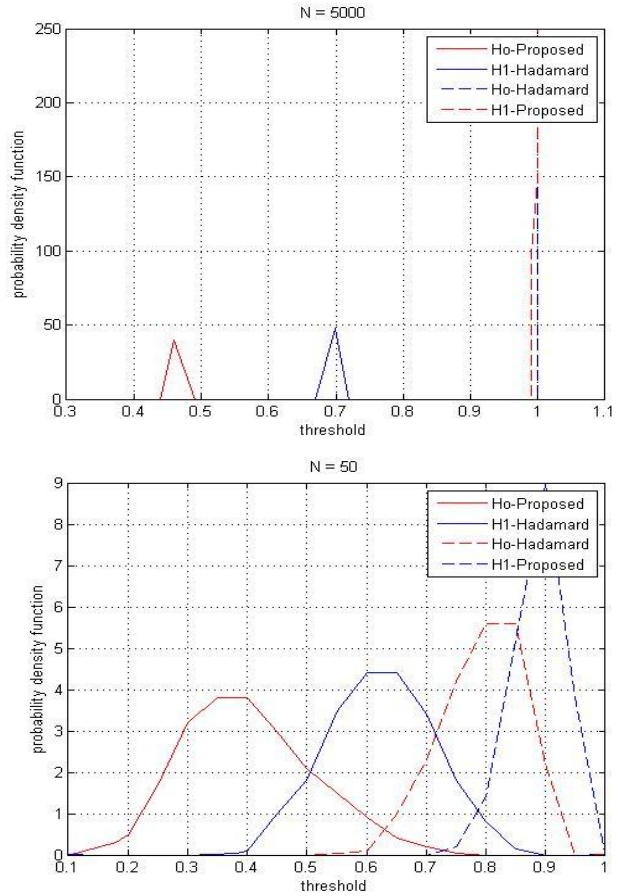

Fig.2:- Probability density function and threshold *M = 4 , d = 3 and SNR = [-2, -3, -4]db.(a) N=5000. (b)N = 50.*

Detection probability:-
False-alarm probability determined by the following proposition,
*Proposition 2:*For any antenna number M and sample number N with $N \geq M$, the two-first-moment Gamma approximation to the PDF of ξ under H_0 is

$$P_0(y) \approx \frac{y\alpha 0-1\beta 0-\alpha 0e-y/\beta 0}{\Gamma(\alpha 0)} \text{ , } y\varepsilon[0,00] \quad (16)$$

Here

$$\alpha 0 = \frac{\mu_0^2}{\nu_0^2} \quad (17a)$$

$$\beta_1 = \frac{\nu_0^2}{\mu_0} \quad (17b)$$

With μ_0 and ν_0 being the second order approximation to the mean of ξ and the first order approximation to the variance of ξ.

It follows from the Proposition 2 that the false-alarm probability is determined as

$$PFA(\Upsilon) \triangleq Prob(\xi < \Upsilon | H_0) = F(\Upsilon;\alpha_0,\beta_0) \quad (18)$$

Given a false-alarm probability $P_{fa,}$ the decision threshold can be obtained by the numerically inverting $F(\Upsilon;\alpha_0,\beta_0)$. That is

$$\Upsilon=F^{-1}(PFA;\alpha_0\beta_0) \quad (19)$$

Here $F^{-1}(.)$ represents the inverse function of the $F(.)$.

And the mapping between the false-alarm probability and detection probability yields in ROC. Hence the analytic ROC formula for the volume-based test is

$$P_d= F[F^{-1=}(P_f;\alpha_0, \beta_0); \alpha_1 , \beta_1] \quad (20)$$

Numerical Results:-

In this section, we are going to the discussion about the simulation results for analytic false alarm and detection probabilities. Moreover, the superiority of the volume-based approach over the representative methods for the spectrum sensing under the IID and non-IID noise conditions are demonstrated.

Analytic False- Alarm and Detection Probability:-

In this one, the accuracy of the analytic formulae for the false alarm and detection probabilities is numerically calculated. To comparison, exact false alarm and detection probabilities, which empirically determined by 10^5 Monte Carlo simulation trials, are presented as well.

In figure 3(a) plots the false-alarm probability versus decision threshold in the presence of IID noise. Here we are using the four antennas, and samples are [100,200,400]. Antennas can represent as *M* and samples can represent as *N*. In figure 3(a) Gamma approximation false-alarm probability is very accurate regarding fitting the empirical false alarm probability for IID noise. The simulation results for Gamma approximate and the empirical false alarm probabilities are depicted in fig3 (b) for $M=6$ and $N=$ [200,400,600]. In this figure, we observed that the Gamma approximation *P*FA is very close to the exact one. This turn implies that the derived false-alarm probability provides the accurate theoretical calculation for practical spectrum sensing.

Let us try the accuracy of the detection probability for the proposed Gamma approximation. Similarly, the exact detection probability empirically determined by 10^5 Monte Carlo simulations is also presented for comparison. The Presence of primary signals, the Rayleigh-fading channel is adopted to evaluate the accuracy of the derived Gamma Approximation P_d.

The Rayleigh-fading situation, the columns of the channel matrix *H* follow a complex Gaussian distribution with zero mean and covariance matrix ϕ due to the correlation between the signals at the receiving antennas which cannot sufficiently space for physical size constraints. The correlated Rayleigh-fading channel model is able precisely to characterize the behavior of the working channel. The (*K, l*) entry of ψ is determined as follows

$$\phi_{kl} = \frac{I_0(\sqrt{k^2-4n^2d_{kl}^2+j\ 4\ nk\sin(\psi)d_{kl}})}{I_0\ (K)} \quad (k\ ,\ l\ =1,..M) \quad (21)$$

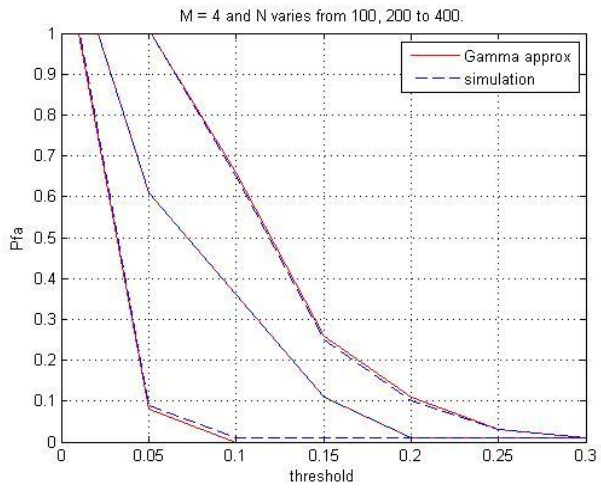

(a)

Where $I_0(.)$ denotes the zero-order modified Bessel function, k controls the width of the angles-of-arrival (AOAs) of the primary signal, impinging upon the receiving antennas of the SU. Which can vary from 0 up to 00 (extremely non-isotropic scattering), $\psi \in [-\pi,\pi)$ represents the mean direction of the AOAs, and d_{kl} stands for the distance, which normalized on the wavelength λ, between the n-th and i-th antennas of the SU.

The figure. 4 demonstrate the numerical results of the single primary signal in the Rayleigh fading channel and under the situation of IID noise.

In this one M =4, *N=100,200 to 300,* and the power of the primary signal set as -5db. It simplified that the derived detection probability can accurately predict the detection performance for the volume-based approach. Fig4 (b) plots the Gamma approximate and exact detection likelihood of the volume-based detection method for IID noise. Here *M=6, N=200,300 to 400,* and the signal power are same as in Fig.4 (a).

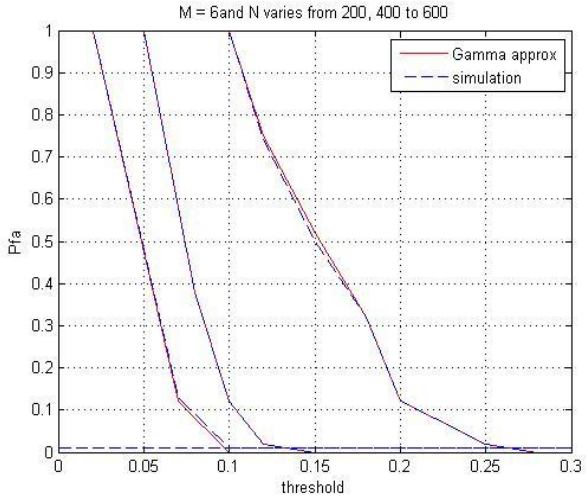

(b)

Fig.3:- False alarm probability versus threshold in IID noise. (a) M =4 and N varies from 100,200 to 400. (b) *M=6* and N range from 200,400 to 600.

The numerical results again validate the efficiency of the derived approximate P_d. These figures are plotting in the Fig. 5.

The numerical results for three primary signals with powers of [-2,-3,-4] dB. And the number of antennas is 4 and the number of samples set as [100, 200, 400] in Fig.5 (a). Here we can observe that the proposed Gamma relative detection probability is quite precise regarding fitting the exact one.
In Fig.5 (b). The number of antennas and some samples set as *M=6* and *N*=[200, 400, 800], respectively. Here in this one, we are observed that the derived P_d is very accurate concerning the predicting the detection performance for the volume-based algorithm.

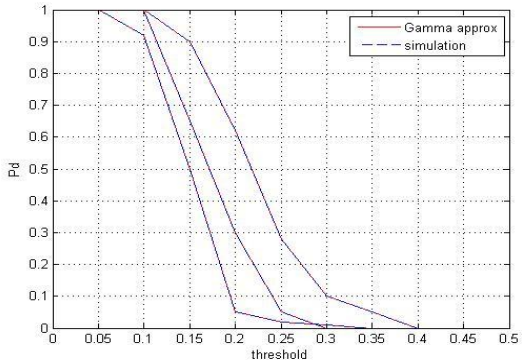

4(a)

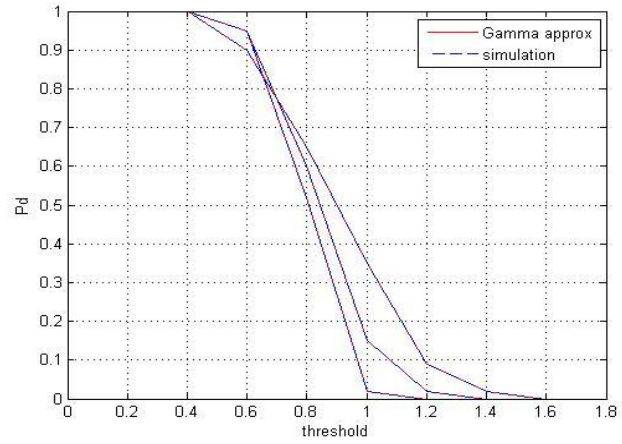

4(b)

Fig.4. Detection probability versus threshold for three primary signals in IID noise. σ_{s1}^2 = -5db.(a) *M=4* and *N* varies from 100, 200 to 300. (b) *M* = 6 and *N* varies from 200, 300 to 400.

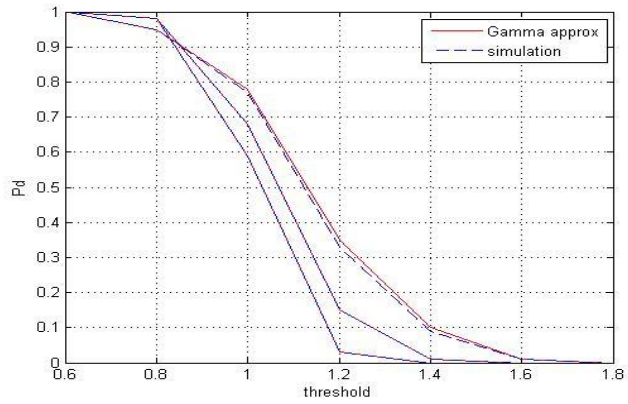

5(a)

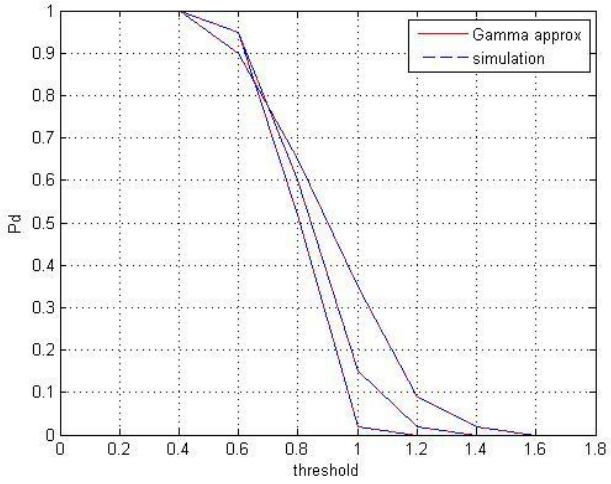

5(b)

Fig.5:- Detection probability versus threshold for three primary signals in IID noise. [σ_{s1}^2 , σ_{s2}^2 , σ_{s3}^2] db. (a) *M= 4* and *N* varies from 100, 200 to 400. (b) *M* = 6 and *N* varies from 200,400 to 800.

Detection Performance:-

Here we have derived robustness as well as the accuracy of the volume-based detection algorithm for complex-valued observed data by comparing its empirical ROC with those other representative methods. In particular, the decision threshold is varied to calculate the false-alarm probability and its corresponding detection probability, leading to the ROC curve, for the purpose of comparison, the numerical results of the John's, AGM (or ST), Hadamard ratio as well as ED detectors are provided. All the numerical results obtained from 10^5 Monte Carlo trials.

The ROC of the volume-based, AGM, John's, Hadamard ratio and Energy detection and IID noise drawn in Figure.6.

In fig. 6(a) where the number of antennas M=4, some samples N=10. The number of primary signals is one, and its power equals to 8 dB, the volume-based approach is superior to the AGM and Hadamard ratio methods but inferior to John's detector which is known to be the locally most powerful invariant test for sphere city. Moreover, all of them are inferior to the actual noise variance based ED approach.

Similarly, in Fig. 6(b) where the number of antennas M = 6, number of samples N = 10, number of primary signals increases to three and their powers are set as $[\sigma_{s1}^2, \sigma_{s2}^2, \sigma_{s3}^2]$ = [5, 2, 0] dB.

It indicates that the volume-based detector surpasses the AGM and Hadamard ratio methods but is not as accurate as John's approach in the scenario of IID noise. However, as the sample number increases to 50, the volume-based algorithm can provide the same accuracy as John's algorithm which has been proved to be the more potent for the small sample case.

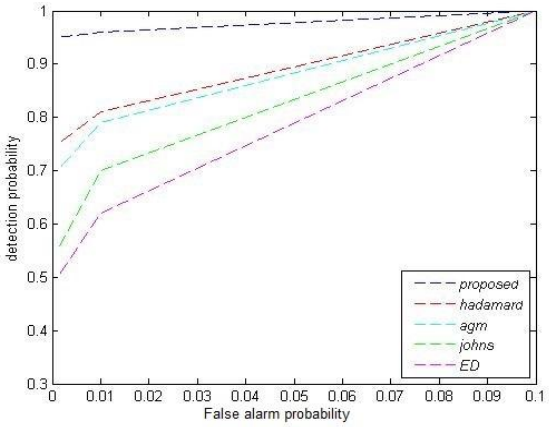

6 (a):-

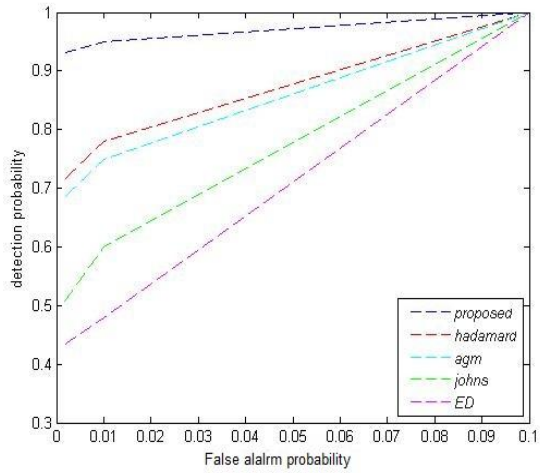

6(b):-

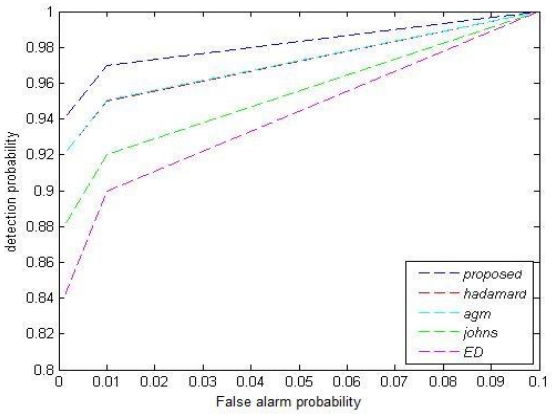

6(c):-

Fig.6:- ROCs of various detectors for Rayleigh fading channel in IID noise. (a) M =4, N =10, d = 1 and σ_{s1}^2 = 8 db, (b) M = 4, N = 10, d = 3 , and $[\sigma_{s1}^2, \sigma_{s2}^2, \sigma_{s3}^2]$ = [5, 2, 0]db, (c) M = 4, N = 50, d =3 ,and $[\sigma_{s1}^2, \sigma_{s2}^2, \sigma_{s3}^2]$ = [0, -3, -5]db.

Similarly in Fig. 7(a) where the numbers of antennas M = 4 number of samples N = 10, primary signal d = 1, and its power equals 8db, and different noise models namely non-IID noise. Under such a sound condition, the volume-based detector is capable of offering the best detection performance among the blind methods. In turn, implies that the volume-based approach is superior to the Hadamard ratio method in accuracy and the AGM and John's schemes in robustness against the deviation of IID noise. In fig. 7(b) where the numbers of antennas M= 4 and number of samples N = 10, primary signals increases to 3 and its powers set as $[\sigma_{s1}^2, \sigma_{s2}^2, \sigma_{s3}^2]$ = [5, 2,0]db, and different noise models namely non-IID noise. Under this condition, we plotted volume-based approach was superior to the Hadamard ratio method in accuracy and the AGM and John's schemes in robustness against the deviation of IID noise. In fig. 7(c) where the numbers of antennas M = 4 and number of samples N = 30, d = 3, and its powers are set as $[\sigma_{s1}^2, \sigma_{s2}^2, \sigma_{s3}^2]$ = [0, -3 , -5] dB, and with non-IID noise. Under this condition, we plotted volume-based approach was superior to the Hadamard ratio method in accuracy and the AGM and John's schemes in robustness against the deviation of IID noise.

Similarly in Fig. 8(a) where the number of antennas M = 6, and some samples N = 10, primary signal d=1, and its power equals 8db, and noise models namely IID. Under such a sound condition, the volume-based method is superior to the AGM and Hadamard ratio schemes but inferior to John's system in detection performance. In fig. 8(b) where the number of antennas M = 6, number of samples N = 10, and primary signals increases to 3 and its powers as set as $[\sigma_{s1}^2, \sigma_{s2}^2, \sigma_{s3}^2]$ = [5, 2, 0] dB, and different noise models namely IID. Under such a sound condition, the volume-based method is superior to the AGM and Hadamard ratio schemes but inferior to John's system in detection performance. In fig. 8(c) where the number of antennas M = 6, some samples N = 50, and primary signals increases to 3 and its powers as set as $[\sigma_{s1}^2, \sigma_{s2}^2, \sigma_{s3}^2]$ =[0, -3 , -5]db with IID noise. Under the situation of these conditions, we plotted volume-based method was superior to the AGM and Hadamard ratio schemes but inferior to John's system in detection performance.

Similarly in Fig. 9(a) where the number of antennas M = 6, number of samples N = 10, the primary signal d=1, and its power equals to 8 dB with non-IID noise. Under these conditions the volume-based detector out-performance the robust Hadamard ratio test and non-robust AGM as well as John's approaches in detection accuracy. In fig. 9(b) where the number of antennas M = 6, number of samples N = 50, and primary signals increases to 3 and its powers as set as $[\sigma_{s1}^2, \sigma_{s2}^2, \sigma_{s3}^2]$ = [5, 2 , 0] dB,, with non-IID noise. Under these conditions the volume-based detector out-performance the robust Hadamard ratio test and non-robust AGM as well as John's approaches in detection accuracy. In fig. 9(c) number of antennas M = 6 , number of samples N = 50 , and primary signals increases to 3 and its power set as $[\sigma_{s1}^2, \sigma_{s2}^2, \sigma_{s3}^2]$ = [0, -3, -5] dB, with non-IID noise. Under this conditions, the volume-based algorithm is even superior to the ED scheme, as drawn in fig. 9(c).

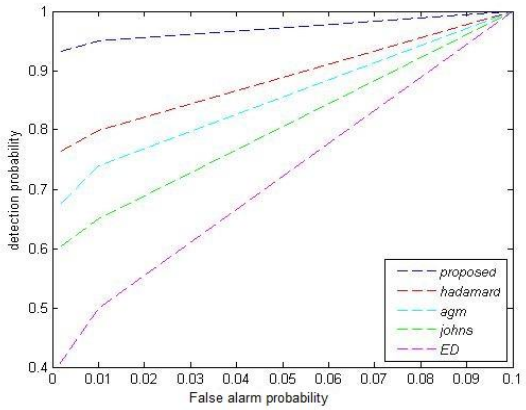

7(a):-

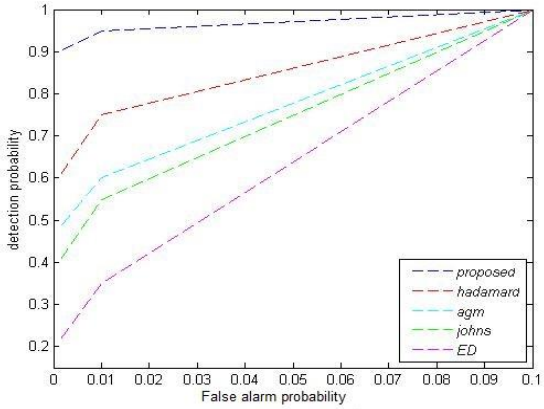

7(b):-

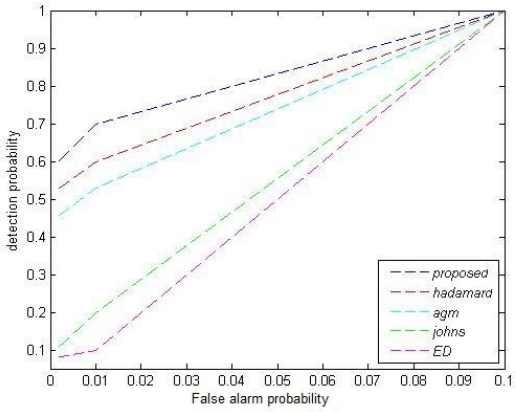

7(c):-

Fig. 7:- ROC of varies detectors for Rayleigh fading channel in non-IID noise.(a) M = 4, N = 10, d = 1 , and σ_{s1}^2 = 8db. (b) M = 4, N = 10, d =3 ,and $[\sigma_{s1}^2, \sigma_{s2}^2, \sigma_{s3}^2]$=[5, 2, 0]db. (c) M = 4 , N = 30 , d = 3 ,and $[\sigma_{s1}^2, \sigma_{s2}^2, \sigma_{s3}^2]$=[0, -3, -5]db.

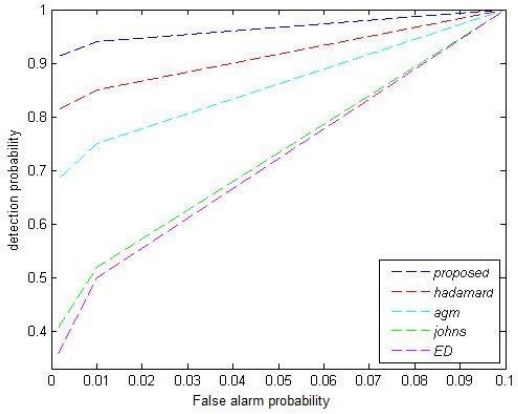

8(a):-

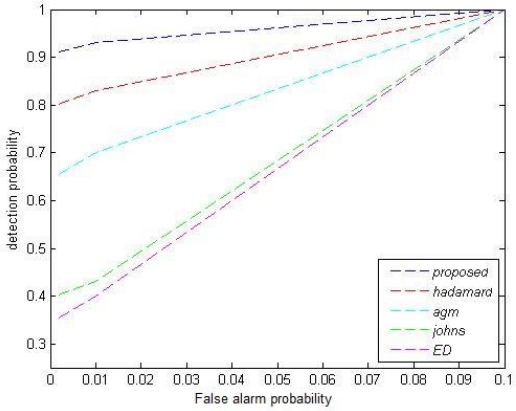

8(b):-

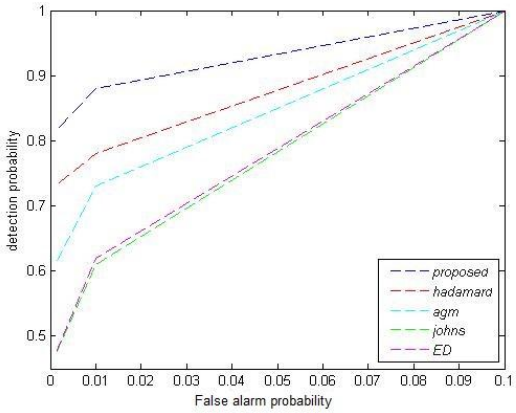

8(c):-

Fig. 8:- ROC s of various detectors for Rayleigh fading channel in IID noise .(a) M = 6, N = 10 , d = 1, and σ_{s1}^2 = 8 db.(b) M = 6, N = 10, d = 3 , and $[\sigma_{s1}^2 , \sigma_{s2}^2 , \sigma_{s3}^2]$ = [5, 2, 0] db.(c) M =6 , N = 50 ,d =3, and $[\sigma_{s1}^2 , \sigma_{s2}^2 , \sigma_{s3}^2]$ = [0, -3, -5]db.

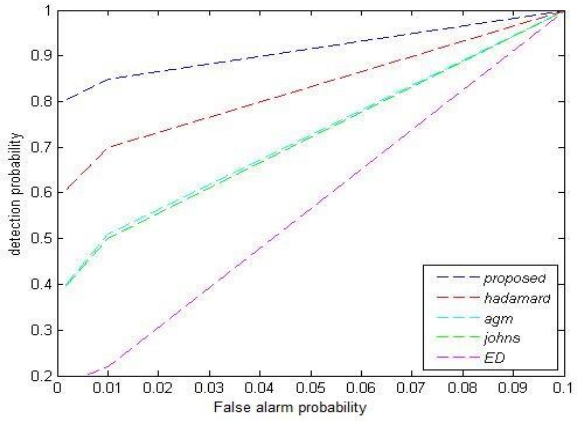

9(a):-

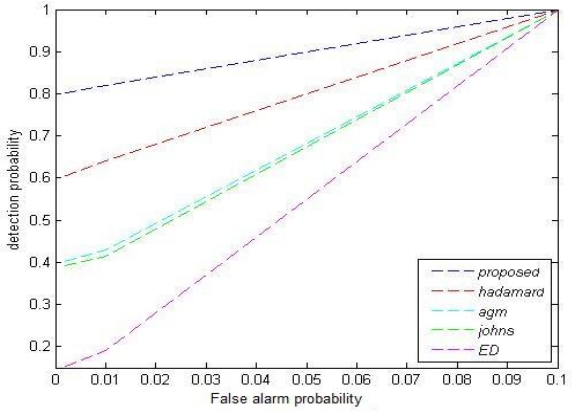

9(b):-

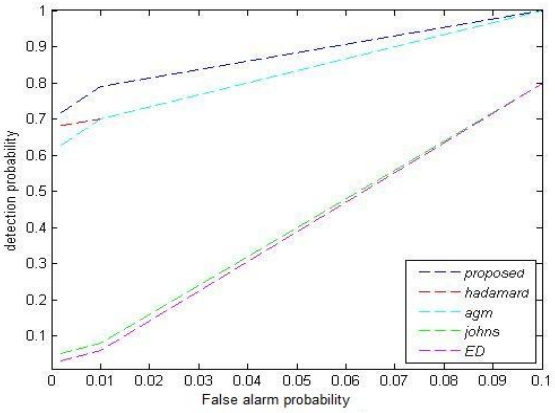

9(c):-

Fig. 9:- .ROC s of various detectors for Rayleigh fading channel in non- IID noise, (a) M = 6, N = 10 , d = 1, and σ_{s1}^2 = 8 db.(b) M = 6, N = 10, d = 3 , and $[\sigma_{s1}^2 , \sigma_{s2}^2 , \sigma_{s3}^2]$ = [5, 2, 0] db.(c) M =6 , N = 50 ,d =3, and $[\sigma_{s1}^2 , \sigma_{s2}^2 , \sigma_{s3}^2]$ = [0, -3, -5]db.

Conclusion:-

The volume-based method has derived for the IID noise; it is providing accurate theoretical threshold calculation and evaluating its sensing performance. Here we are taking first and second moments of signal active, signal in a current hypothesis; we can employ the Moment-matching method accurately derive the Gamma distribution.

By computing the exact first and second moments of the test statistic under the current signal hypothesis, we are capable of approximating the Gamma distribution for the volume-based test static, ending up with an accurate analytic expression for the detection probability.

References:-

1. Bruce A. Fette, "Cognitive Radio Technology" , Newnes publications, 2nd edition,2009.
2. S. Haykin, "Cognitive Radio: Brain-Empowered Wireless Communications", IEEE J.Sel. Areas Communication., vol.23, no. 2, pp.201-220, Feb.2005.
3. Mansi Subhedar and Gajanan Birajdar "Spectrum Sensing Techniques in Cognitive Radio networks: a survey" International Journal of Next-Generation Networks (IJNGN) Vol.3, No.2, June 2011.
4. L. Wei and O. Tirkkonen, "Spectrum sensing in the presence of multiple primary users," IEEE Trans. Commun., vol. 60, no. 5, pp. 1268–1277, May 2012.
5. Ian F. Akyildiz, Brandon F. Lo∗, Ravi Kumar Balakrishnan, "Cooperative Spectrum Sensing in Cognitive Radio Networks: A Survey" Physical Communication 4- 40–62, 2011.
6. S. Zarin, T.J. Lim, "Composite hypothesis testing for cooperative spectrum sensing in cognitive radio," in Proc. of IEEE ICC, pp.1-5, 2009.
7. Ruiling Chen, Jung-Min Park, and Kaigui Bian, 'Robust Distributed Spectrum Sensing in Cognitive Radio Networks", IEEE INFOCOM 2008.
8. S. S. M. Biguesh and M. Gazor, "Optimal training sequence for MIMO wireless systems in colored environments," IEEE Trans. Signal Process., vol. 57, no. 8, pp. 3144-3153, Aug. 2009.
9. Sheikhi and A. Zamani, "Coherent detection for MIMO radars," in Proc. IEEE Radar Conf., 2007.
10. L.Wei. P. Dharmawansa,.and O. Tirkkon, "Multiple primary user spectra sensing in the low SNR regime," IEEE Trans. Commun., vol.61, no.5. pp.172-1731, May 2013.
11. R. Zhang, T. Lim, Y.C, Liang and Y. Zeng, "Multi-antenna based spectrum sensing for cognitive radio: A GLRT approach," IEEE Trans.commun., vol.58,.no.1. pp.84-88, jan.2010.
12. P. Wang, J. Fang, N. Han, and H. Li, "Multi antenna-assisted spectrum sensing for cognitive radio," IEEE Trans. Veh. Technol., vol. 59, no. 4, pp. 1791–1800, May 2010.
13. Taherpour, M. Nasiri-Kenari, and S. Gazor, "Multiple antenna spectrum sensing in cognitive radios," IEEE Trans. Wireless Commun., vol. 9, no. 2, pp. 814–823, Nov. 2010.
14. Q. T. Zhang, "Theoretical performance and thresholds of multitaper method for spectrum sensing", IEEE Trans. Signal process vol. 5, no.1. pp.49-55, Feb,2011.
15. F. F. Digham, M. S. Alouini, and M. K. Simon, "On the energy detection of unknown signals over fading channels," IEEE Trans. Commun., vol. 55, no. 1, pp. 21–24, Jan. 2007.
16. Y. Zeng, C. L. Koh, and Y.-C. Liang, "Maximum eigenvalue detection: Theory and application," in Proc. IEEE ICC, Beijing, China, pp. 4160–4164, May 2008.
17. Q. T. Zhang, "Theoretical Performance and Thresholds of the multitaper method for spectrum sensing," IEEE Trans. Veh. Technol., vol. 60, no. 5, pp. 2128–2138, Jun. 2011.
18. Lei Huang, Cheng Qian, Yuhang Xiao, Q. T. Zhang, "Performance Analysis of Volume-Based Spectrum Sensing for Cognitive Radio" IEEE Transactions on Wireless Communications, VOL. 14, NO. 1, JANUARY 2015.